Polymer 53 (2012) 3726–3734

Contents lists available at SciVerse ScienceDirect

Polymer

journal homepage: www.elsevier.com/locate/polymer

Synthesis of linear isotactic-rich poly(*p*-methylstyrene) *via* cationic polymerization coinitiated with $AlCl_3$

Bei-te Li, Yi-xian Wu*, Hong Cheng, Wen-hong Liu

State Key Laboratory of Chemical Resource Engineering, Key Laboratory of Carbon Fiber and Functional Polymers (Ministry of Education), Beijing University of Chemical Technology, Beijing 100029, China

ARTICLE INFO

Article history:
Received 21 September 2011
Received in revised form
31 March 2012
Accepted 5 April 2012
Available online 8 May 2012

Keywords:
Cationic polymerization
Styrene
Stereoregularity

ABSTRACT

Cationic polymerizations of *p*-methylstyrene (*p*MS) with $H_2O/AlCl_3$/triphenylamine (TPA) or triethylamine (TEA) initiating system were carried out in mixed solvents of *n*-hexane and dichloromethane at −80 ~ −50 °C. The effects of TPA or TEA concentration, solvent polarity, polymerization temperature and time on monomer conversion, number-average molecular weight (M_n), molecular weight distribution (MWD, M_w/M_n), stereoregulatity and crystallinity of poly(*p*-methylstyrene) (P*p*MS) were investigated. The stereospecific cationic polymerization of *p*-methylstyrene could be achieved and high molecular weight (M_n = 116,000 ~ 436,000 g mol^{-1}) polymers with isotactic-rich segments (more than 75% of meso dyad) along macromolecular chains could be successfully synthesized. A possible mechanism for stereospecific cationic polymerization of *p*MS was proposed. The propagation proceeded *via* the dominant back-side attack and insertion of monomer from the growing ion paired species. The steric course of propagation was mainly determined by the tightness of the growing ion paired species and steric hindrance in counteranion. The resulting isotactic-rich P*p*MS could form crystal morphology with 10 ~ 30 μm in size by flow-induced crystallization under pressure at 180 °C. A possible model for the aligning mechanism was sketched to describe crystallization and to explain the multi-melting peaks and lower glass transition temperatures of P*p*MS. This is the first example of stereospecific cationic polymerization of *p*-methylstyrene to get crystallizable polymers with such high molecular weights and isotacticity.

© 2012 Published by Elsevier Ltd.

1. Introduction

Stereoregularity is one of the most important factors to affect seriously the crystallinity and physical properties of polymers. Styrene and its derivatives such as *p*-methylstyrene are capable of undergoing the controlled/living cationic polymerization coinitiated by various Lewis acids, such as BCl_3, $SnCl_4$, $TiCl_4$ or $FeCl_3$ or $B(C_6F_5)_3$ [1–12]. However, it is really rather difficult to achieve high stereoregulation in cationic polymerization for the lack of controlling the stereochemistry. Namely, the stereoregularity control is generally poor in cationic polymerization and only few stereoregular polymers such as [poly(3-methyl-1-butene)], polybenzyls and poly(vinyl ether)s could be prepared [13–21]. The efforts for stereoregulation and stereochemistry have been made in cationic polymerization of vinyl ether monomers [15–22]. In the cationic polymerization of isobutyl vinyl ether, the unsubstituted counterparts ($TiCl_4$, $SnCl_4$, etc.) gave nearly atactic products while bis[(2,6-diisopropyl)phenoxy] titanium dichloride gave isotactic-rich polymers with a meso dyad (m) of 90–92% in the presence of a bulky pyridine (2,6-di-*tert*-butyl-4-methylpyridine) under similar conditions [20]. Mechanisms have also been proposed for the formation of isotactic and syndiotactic enchainments in cationic polymerization [19–21]. The front-side attack of monomer leads to the formation of syndiotactic polymer, and on the other hand, the back-side attack of momomer leads to the formation of isotactic polymer [19–21]. The tacticity of poly(vinyl ether) was influenced by Lewis acids or counteranions, substituents of monomers, solvent polarity and temperature [20–25].

It has been reported that the polymerization of linear olefins using the equivalent of 0.1 mol excess $AlCl_3$ in ionic liquid 1-butyl-3-methylimidazolium tetrachloroaluminate ([bmim][$AlCl_4$]) in the presence of ethyl aluminum dichloride resulted in the formation of atactic oligomers with large molecular weight distribution [26]. Very recently, the cationic polymerizations of styrene in ionic liquid have been reported to produce polymers with a slight predominance of syndiotactic sequences but no information on crystalline of polystyrene was presented [27,28]. The controlled cationic

* Corresponding author.
E-mail address: yxwu@263.net (Y.-X. Wu).

0032-3861/$ – see front matter © 2012 Published by Elsevier Ltd.
doi:10.1016/j.polymer.2012.04.003

polymerization of styrene was achieved using bisoxalatoboric acid as an initiator in ionic liquid to obtain polymers with low molecular weights (M_w < 3000 g mol^{-1}) and a mixture of polymer triad sequences (syndiotactic, isotactic, and atactic) with a predominance (~43%) of syndiotactic sequences (rr) could be obtained [27]. The cationic polymerization of styrene was also conducted in supercritical CO_2 and/or [bmim][PF_6] to produce low molecular weight polymers having a higher intensity for the rr triad centered at 145 ppm related to syndiotactic sequences or sometimes a slight tendency for the predominance of isotactic sequences [28].

In order to increase molecular weight, enhance stereoregularity and improve crystallinity, the H_2O/$AlCl_3$/triphenylamine (TPA) or triethylamine (TEA) initiating systems have been developed to initiate the stereospecific cationic polymerization of *p*-methylstyrene and to prepare crystallizable poly(*p*-methylstyrene) with high molecular weight in this paper. The effects of TPA concentration, solvent polarity, polymerization temperature and time on molecular weight, molecular weight distribution and crystallizability of poly(*p*-methylstyrene) products were examined. A possible mechanism was proposed for the stereospecific cationic polymerization of *p*-methylstyrene and a model for the aligning mechanism was also sketched to describe the flow-induced crystallization of poly(*p*-methylstyrene).

2. Experimental section

2.1. Materials

p-Methylstyrene (*p*MS, ACROS Company, purity > 98%) was dried by introduction of CaH_2 and freshly distilled under reduced pressure before use. *n*-hexane (*n*-Hex, Beijing Houhui Chemical Co.), CH_2Cl_2 (Beijing Houhui Chemical Co.) and tetrahydrofuran (THF, AR, Beijing Yili Fine Chemical Co.) were distilled from CaH_2 before use. Triphenylamine (TPA, ACROS Company, purity > 99%) was dried under vacuum before use. Anhydrous aluminum trichloride ($AlCl_3$, ACROS Company, purity > 99%, packaging under nitrogen), triethylamine (TEA, Tianjin Fuchen Chemical Reagents, purity > 99%) and ethanol (AR, Beijing Yili Fine Chemical Co.) were used without further purification.

2.2. Procedures

All the manipulation, reactions and cationic polymerizations of *p*-methylstyrene were carried out under dry nitrogen in baked glassware equipped with three-way stopcocks. Specific reaction conditions are listed in the Figure captions. A representative procedure was described as follows: The monomer solution in the mixture of CH_2Cl_2 and *n*-Hex was prepared in a chilled 1000 mL round-bottom flask at −80 °C. The monomer solution was airtightly transferred to the 20 mm × 200 mm test tube (polymerization reactor) *via* a 20 mL volumetric pipette and cooled at the desired reaction temperature for more than 30 min. The solutions of H_2O, triphenylamine or triethylamin and $AlCl_3$ in CH_2Cl_2 were introduced through syringes into the above *p*-methylstyrene solutions to initiate the polymerization for a given time and terminated by ethanol containing 1% NaOH. The resultant polymer was purified two times by re-precipitation from hexane/ethanol, washed with water and ethanol and finally dried under vacuum at 45 °C to constant weight. The monomer conversion was determined gravimetrically. The control sample of atactic poly(*p*-methylstyrene) (P*p*MS) with high molecular weight (M_n = 225,000 g mol^{-1}, M_w/M_n = 2.7) in the DSC experiments was synthesized *via* bulk free radical polymerization of *p*-methylstyrene at 120 °C.

2.3. Measurements

The H_2O concentration in the polymerization system was monitored electrochemically with an SF-6 water determination apparatus (Shandong Zibozifen Instrument Co.) in conjunction with a Karl-Fischer reagent for coulometric titration according to the method described previously [29]. The number-average molecular weight (M_n), weight-average molecular weight (M_w) and molecular weight distribution (MWD, M_w/M_n) of poly(*p*-methylstyrene) were measured by gel permeation chromatography (GPC) system (Waters 515–2410) equipped with four Waters styragel columns connected in the following series: 500, 10^3, 10^4, and 10^5, which were connected to a Waters-1515 isocratic HPLC pump and a Waters-2414 refractive index detector in tetrahydrofuran at 30 °C. The columns were calibrated against standard polystyrene samples. THF was eluted at a flow rate of 1.0 mL min^{-1}.

The theoretical molecular weight ($M_{n,\mathrm{theo}}$) was calculated according to the following equation:

$$M_{n,\mathrm{theo}} = [p\mathrm{MS}]_0 \times \mathrm{conversion} \times 118/[\mathrm{H_2O}]_0$$

The initiation efficiency (I_{eff}) was calculated according to the following equation:

$$I_{\mathrm{eff}} = M_{n,\mathrm{theo}}/(M_{n,\mathrm{exp}} \times \mathrm{conversion})$$

The film of poly(*p*-methylstyrene) was prepared on slide under a constant pressure of 10 kg cm^{-2} for about 30 s at temperature of 180 °C and then taken out and kept at room temperature for 10 min. The micrograph of polarized optical microscope (POM) on poly(*p*-methylstyrene) film was recorded using Leitz SM-LUX-POL POM. The film of poly(*p*-methylstyrene) for DSC measurement was formed as same as the film for POM measurement, and was characterized by the Q200 MDSC (TA Instruments Company) at a scan rate of 5 K min^{-1} under nitrogen. Sample for TEM characterization was sectioned using a F6C + FC6 ultramicrotome at −60 °C using a diamond knife to produce section samples with around 100 nm thickness. Specimen was placed on 400-mesh Cu grids without staining and TEM characterization was performed on a HITACHI-800 transmission electron microscope at 200 kV. The ^{13}C NMR spectra were collected on a Bruker AV600 MHz spectrometer for 4 h in *o*-dichlorobenzene at 25 °C under conditions of pulse delay of 6.5 usec, acquisition time of 0.62 s and number of transients of 5500. The proportions of mmmm pentad, mm triad and m dyad were determined on the basis of the integrals of characteristic signals in the quantitative ^{13}C NMR characterization [30].

$$P(\mathrm{mmmm}) = \frac{A_{143.6}}{A_{143.6} + A_{143.2} + A_{142.8}} \times 100\%$$

$$P(\mathrm{mm}) = \frac{A_{143.6} + A_{143.2}}{A_{143.6} + A_{143.2} + A_{142.8}} \times 100\%$$

$$P(\mathrm{m}) = \frac{A_{143.6} + A_{143.2} + \frac{A_{142.8}}{2}}{A_{143.6} + A_{143.2} + A_{142.8}} \times 100\%$$

wherein, *P*(mmmm), *P*(mm) and *P*(m) are the proportion of mmmm pentad, mm triad and m dyad respectively; $A_{143.6}$, $A_{143.2}$ and $A_{142.8}$ are the integrals of resonances at 143.6 ppm, 143.2 ppm and 142.8 ppm respectively in ^{13}C NMR spectra by multi-peak fitting.

3. Results and discussion

3.1. Cationic polymerization of pMS with H_2O/$AlCl_3$/triphenylamine initiating system

The control experiment of cationic polymerizations of *p*-methylstyrene (*p*MS) with H_2O/$AlCl_3$ initiating system was

conducted in the absence of amine at −80 °C for comparison. The GPC curve with the data of molecular weights and molecular weight distribution for the control experiment in the absence of amine is given in Fig. 1(a). The resulting poly(*p*-methylstyrene) (P*p*MS-0) in the control experiment has relatively low number-average molecular weight (M_n = 95,000 g mol^{-1}) and broad molecular weight distribution (MWD, M_w/M_n = 4.5). Then, the cationic polymerizations of *p*MS with $H_2O/AlCl_3$/triphenylamine (TPA) initiating system were carried out in *n*-hexane/CH_2Cl_2 mixture (60/40, v/v) at −80 °C. All the resulting P*p*MS products are soluble in tetrahydrofuran and butanone. Fig. 1(b) shows the GPC traces of P*p*MS products (P*p*MS-1, P*p*MS-2) obtained at different monomer concentrations and polymerization times of 0.3 M, 0.2 min and 0.5 M, 30 min, respectively. The cationic polymerization proceeded rapidly to reach 87.9% of monomer conversion within 0.2 min even at low monomer concentration ([*p*MS] = 0.3 M) and P*p*MS-1 with high M_n of 176,000 g mol^{-1} could be obtained. As shown in Fig. 1, all the monomer nearly completed conversion and P*p*MS-2 with higher molecular weight (M_n = 276,000 g mol^{-1}) could also be synthesized at [*p*MS] = 0.5 M. The intermolecular alkylation did not occur under monomer starved conditions due to the existence of −CH_3 at the *para*-position of phenyl group. The fact that molecular weights of P*p*MS products obtained at different polymerization time almost kept unchanged after monomer consumption further proved the absence of intermolecular alkylation. Therefore, the experimental molecular weights ($M_{n,exp}$) of these two polymers are much higher than the corresponding theoretical values ($M_{n,theo}$) of 35,000 g mol^{-1} for P*p*MS-1 and 73,000 g mol^{-1} for P*p*MS-2 respectively, which is attributed to the relatively low initiation efficiency (I_{eff}) of 0.23–0.26 from initiator (H_2O). The monomodal but broad molecular weight distributions (M_w/M_n = 3.9 and 4.3) are probably due to the slow initiation and rapid propagation.

P*p*MS-0, P*p*MS-1 and P*p*MS-2 were characterized by polarized optical microscope (POM) and the corresponding POM images are shown in Fig. 2. It can be clearly observed that almost no crystalline formed for P*p*MS-0, while P*p*MS-1 and P*p*MS-2 could form crystal morphology with 10–30 μm in size under the same flow-induced conditions. Compared to P*p*MS-1 with 38% of mmmm pentad, the crystallizability of P*p*MS-2 with only slightly lower mmmm pentad (37%) increased with increasing its molecular weight all other factors almost being equal. Fig. 3 presents the internal structure of the crystals of P*p*MS-2 characterized by transmission electron microscope (TEM). It can bee clearly seen from TEM images of P*p*MS-2 that there exist many fiber-like lamellar crystallines emerged in P*p*MS matix resulted from the stereoregular sequences along polymer chains. The orientation degree increased with stereoregularity and length of the stereoregular sequence segments in P*p*MS chains. It can be further observed that both the well-ordered long fiber-like crystallines in Fig. 3(A) and ill-organized short fiber-like crystallines in Fig. 3(B) existed in the crystallizable polymer, leading to creation of the crystal morphology with various sizes and shapes, as shown in Fig. 2. And the variform crystal morphology could also give rise to the different thermodynamics of the crystalline regions. Therefore, it can be induced that the short isotactic sequences along polymer chain in the absence of external TPA were difficult to form obvious crystalline under the same flow-induced crystallization conditions.

In order to confirm the crystallizability of P*p*MS products obtained by cationic polymerization, P*p*MS-1 and P*p*MS-2 were further characterized by differential scanning calorimetry (DSC) and the representative DSC curves are given in Fig. 4. The atactic poly(*p*-methylstyrene) (P*p*MS) with high molecular weight (M_n = 225,000) was used as a reference for DSC measurement and the DSC curve of atactic P*p*MS is also given in Fig. 4. As shown in Fig. 4, the atactic P*p*MS had a glass transition temperature (T_g) of *ca.* 110 °C, which is near to the theoretical value (*ca.*116 °C). And no melting temperature (T_m) was detected of the atactic P*p*MS in the DSC measurement. Compared to the atactic P*p*MS, it can be seen from Fig. 4 that the high molecular weight P*p*MS-1 and P*p*MS-2 obtained by cationic polymerization present much lower T_g at *ca.* 93 and 94 °C than that of *ca.* 110 °C for atactic P*p*MS with sufficient high molecular weight. T_g is dependent on average degree of polymerization for many polymers including polystyrene and poly(α-methyl styrene) [31]. It has be also recognized that T_g of polymer increases with its molecular weight to a certain extent and then keeps unchanged when the molecular weight is high enough. Therefore, lower T_g for very high molecular weight P*p*MS-1 and P*p*MS-2 may be attributed to the relatively short sequences of atactic segments and stereoregular segments along macromolecular chains of P*p*MS. Moreover, the multiple endothermic peaks ranging from 159 °C to 227 °C for melting temperatures (T_ms) of crystals could be also observed in Fig. 4, which is attributed to the broad crystalline segment distribution and variform crystal morphology [32,33].

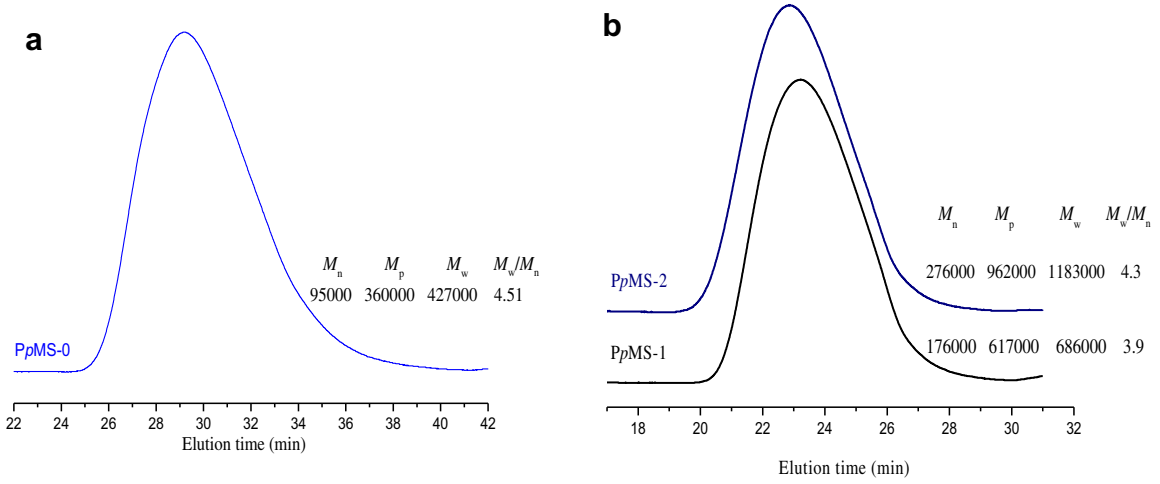

Fig. 1. GPC curves of poly(*p*-methylstyrene) obtained by cationic polymerization with $H_2O/AlCl_3$ initiating system in the absence and presence of TPA. (a) P*p*MS-0: [$AlCl_3$] = 3.8 mM, [H_2O] = 1.23 mM, [*p*MS] = 0.5 M, T_p = −80 °C, $V_{n-Hex}/V_{CH_2Cl_2}$ = 6/4. t_p = 30 min, conversion = 99.9%; (b) [$AlCl_3$] = 3.8 mM, [TPA] = 1.9 mM, T_p = −80 °C, $V_{n-Hex}/V_{CH_2Cl_2}$ = 6/4. P*p*MS-1: [H_2O] = 0.90 mM, [*p*MS] = 0.3 M, t_p = 0.2 min, conversion = 87.9%, $M_{n,theo}$ = 35,000 g mol^{-1}, I_{eff} = 0.23; P*p*MS-2: [H_2O] = 0.81 mM, [*p*MS] = 0.5 M, t_p = 30 min, conversion = 99.9%, $M_{n,theo}$ = 73,000 g mol^{-1}, I_{eff} = 0.26.

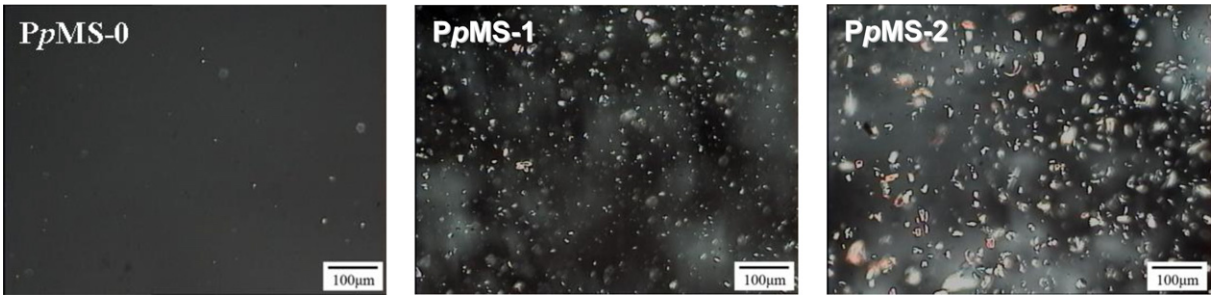

Fig. 2. POM images of P*p*MS-0, P*p*MS-1 and P*p*MS-2 after flow-induced crystallization under pressure. Pressure = 10 kg cm^{-1}, T_c = 180 °C, other conditions are shown as in Fig. 1.

In order to further investigate the stereoregularity and configuration of P*p*MS, the polymers were examined by ^{13}C NMR spectroscopy and the representative ^{13}C NMR spectra are given in Fig. 5. The stereoregularity of P*p*MS can be determined from the intendity ratios of the characteristic peaks of the aromatic C_1 carbon in the region of 142–144 ppm for isotactic, atactic and syndiotactic sequences correspondingly. The ^{13}C NMR spectra of P*p*MS in Fig. 5 present the main characteristic resonance signals at δ = 143.6, 143.2, and 142.8 ppm. The resonance at δ = 143.6 ppm is assigned to the mmmm pentad of isotactic sequence. The resonance at δ = 143.2 ppm is assigned to the rmmr triad, and the resonance signal at δ = 142.8 ppm is for mmrm and mmrr triad or rmrm rrmr dyad [34]. The characteristic resonance signal at δ = 142.3 ppm for rrrr pentad was undetectable, indicating that there is hardly long syndiotactic sequences along polymer chains [35]. The proportions of mmmm pentad, mm triad and m dyad in P*p*MS-1 was determined to be 37%, 62% and 81% respectively [30]. The proportion of mmmm pentad peak was almost independent on polymerization time and monomer conversion since the proportions of mmmm pentad, mm triad and m dyad in P*p*MS-2 was determined to be 38%, 62% and 81% respectively. However, atactic PS has only 7% of mmmm pentad and 45% of m dyad. Therefore, the stereospecific polymerization of *p*-methylstyrene with $H_2O/AlCl_3$/TPA initiating system could be achieved to create the crystallizable polymers with high meso contents of more than 80%. These experimental observations show that character and properties of P*p*MS may be modified by its tacticity, sequence distribution and molecular weight, which may lead to developing a new series of P*p*MS advanced materials by mediating the tacticity and sequence distribution.

3.2. Effect of TPA concentration

The cationic polymerization of *p*-methylstyrene initiated with $H_2O/AlCl_3$/TPA were further carried out at various concentrations of TPA in *n*-hexane/CH_2Cl_2 (6/4, v/v) at −80 °C by keeping [$AlCl_3$] at 3.8 mM. The GPC traces and the corresponding data for the resulting polymers are given in Fig. 6. The monomer conversions decreased slightly from 99.2% to 83.7% with increasing concentration of TPA from 1.9 nM to 2.7 mM while greatly decreased to 28.5% when concentration of TPA was further increased to 2.9 mM. $M_{n,s}$ of the resulting polymers with high yields increased gradually from 116,000 g mol^{-1} to 286,000 g mol^{-1}, MWD narrowed and polydispersity decreased from 4.1 to 2.8 with increasing concentration of TPA from 1.9 mM to 2.7 mM. From these experimental data and the GPC traces in Fig. 6, it can be clearly observed that the portion of low molecular weight fraction decreased with increasing TPA concentration and molecular weight at peak (M_p) increased, indicating that the side reactions of chain termination or chain transfer reaction could be greatly decreased. Thus, the mechanistic roles of TPA were mainly to decrease the cationicity of growing species, to increase the stability of growing species and steric hindrance in counteranions, resulting in decreases in the polymerization rate and molecular weight distribution while increases in the average molecular weights. The polymerization proceeded *via* the propagation from ion pair species. The monomer insertion on the growing ion pair species was limited by the distance (tightness) between cations and counteranions in growing ion pair species, and the steric hindrance from counteranions as well, resulting in formation of some stereoregular segments. “Back-side attack” means that the incoming monomer attacks the carbonium ion on the side opposite from the counterion, and “front-side attack” means the incoming monomer attacks the carbonium ion on the same side as the counteranion [24]. Due to steric interactions within the ion pair, the side of the plane on which the counterion is positioned is such that main back-side attack leads to an isotactic sequence. Therefore, the isotactic-rich poly(*p*-methylstyrene) products, such as P*p*MS-1, P*p*MS-2, P*p*MS-3 or P*p*MS-4, with very high molecular weight and dyad m of more than 80% could be synthesized *via* back-side attacking of monomer to propagating

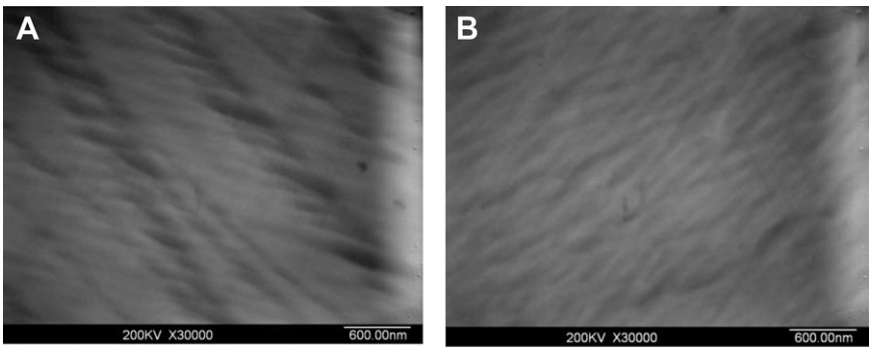

Fig. 3. TEM images of P*p*MS-2 after flow-induced crystallization under pressure. A: well-ordered long fiber-like crystallines; B: ill-organized short fiber-like crystallines; pressure = 10 kg cm^{-1}, T_c = 180 °C, other conditions are shown as in Fig. 1.

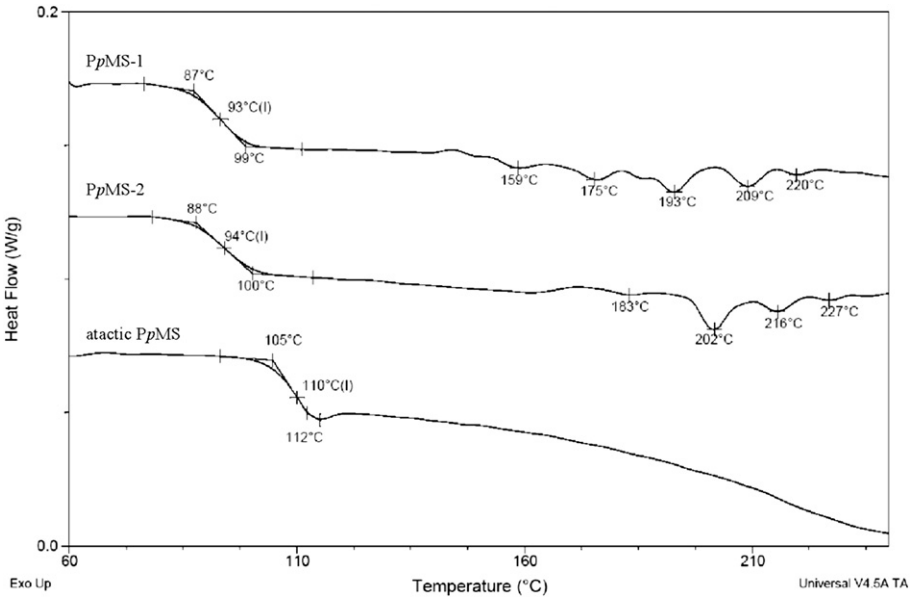

Fig. 4. DSC curves of P*p*MS-1, P*p*MS-2 and atactic P*p*MS after flow-induced crystallization under pressure. Pressure = 10 kg cm^{-1}, T_c = 180 °C, other conditions are shown as in Fig. 1.

cations at appropriate TPA concentrations, i.e. [TPA] = 1.9–2.3 mM. However, excess TPA resulted in a slight decrease of the stereoregularity of segments along polymer chain for *P*(mmmm) decreasing from 38% to 32%, as shown P*p*MS-3 and P*p*MS-6 in Fig. 6.

3.3. Effect of solvent polarity

The polarity of solvent is a crucial factor for salvation and character of active centers in ionic polymerization. The effect of solvent polarity on cationic polymerization of *p*MS with $H_2O/AlCl_3$/TPA initiating system was conducted by changing the volume ratios of *n*-hexane/CH_2Cl_2 from 8/2 to 0/10 while keeping other conditions constant. The solvent polarity decreased with increasing *n*-hexane fraction in *n*-hexane/CH_2Cl_2 mixtures. The tightness of the propagating ion pairs increased with decreasing polarity of solvent in polymerization systems, leading to an increase in possibility for monomer insertion *via* back-side attacking to the growing cations. As shown in Fig. 7, the proportions of mmmm pentad, mm triad and m dyad in poly(*p*-methylstyrene) products increased from 27% to 40%, from 43% to 64% and from 72% to 82% respectively with increasing $V_{n-Hex}/V_{CH_2Cl_2}$ from 0 (0/10) to 4 (8/2). T_g decreased from 99 to 92 °C while melting enthalpy increased from 1.7 to 8.9 J g^{-1} with decreasing solvent polarity, which may be attributed to the increasing possibility of back-side attack of monomer to the more contact growing ion pairs for propagation. Namely, the isotactic propagation is preferred in ion pair growing

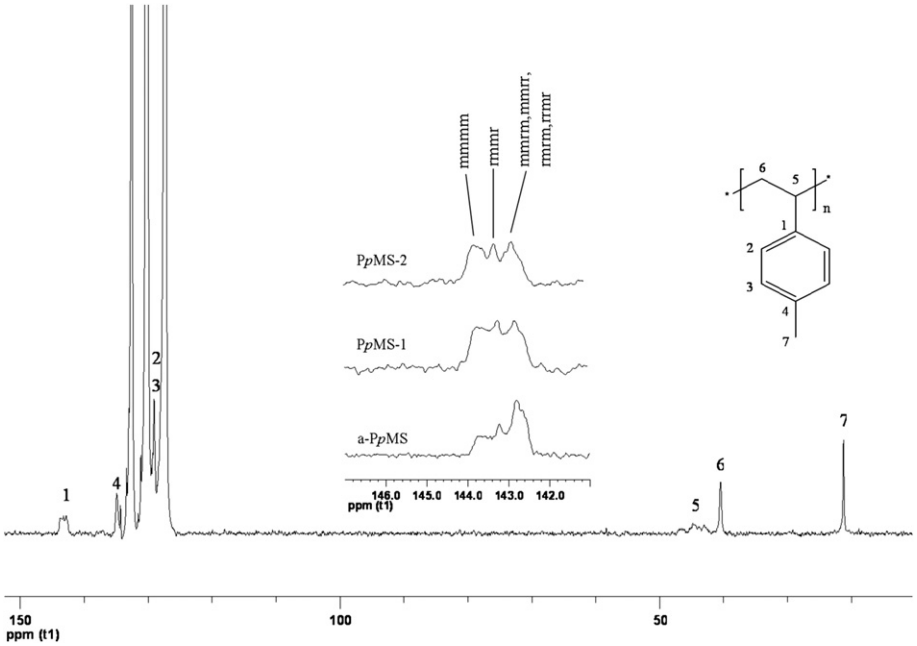

Fig. 5. ^{13}C NMR spectra of P*p*MS-1, P*p*MS-2 and atactic P*p*MS. P*p*MS-1: *P*(mmmm) = 38%, *P*(mm) = 62%, *P*(*m*) = 81%; P*p*MS-2: *P*(mmmm) = 37%, *P*(mm) = 62%, *P*(m) = 81%; atactic P*p*MS: *P*(mmmm) = 15%, *P*(mm) = 32%, *P*(m) = 66%. The full spectrum corresponds to P*p*MS-1.

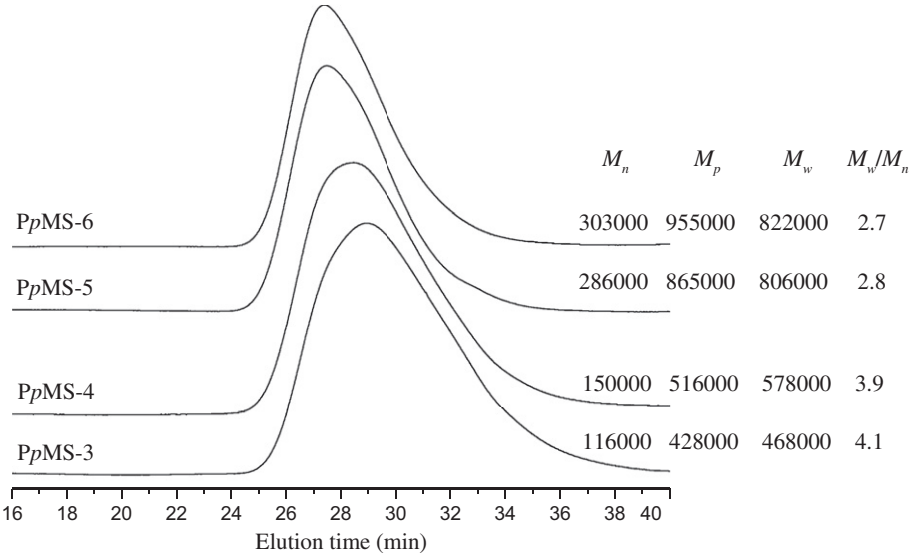

Fig. 6. GPC traces of poly(*p*-methylstyrene) obtained in different TPA concentrations: [PMS] = 0.5 M, [$AlCl_3$] = 3.8 mM, [H_2O] = 1.45 mM; $V_{n-Hex}/V_{CH_2Cl_2}$ = 6/4; T_p = −80 °C; t_p = 30 min. PpMS-3: [TPA] = 1.9 mM, Conv% = 99.2%, *P*(mmmm) = 38%, *P*(mm) = 62%, *P*(*m*) = 81%; PpMS-4: [TPA] = 2.3 mM, Conv% = 98.2%, *P*(mmmm) = 37%, *P*(mm) = 62%, *P*(m) = 81%; PpMS-5: [TPA] = 2.7 mM, Conv% = 83.7%, *P*(mmmm) = 34%, *P*(mm) = 58%, *P*(m) = 79%; PpMS-6: [TPA] = 2.9 mM, Conv% = 28.5%, *P*(mmmm) = 32%, *P*(mm) = 53%, *P*(m) = 76%.

ends in solvent with lower polarity, which is similar to the research results in vinyl ether polymerizations reported by Higashimura and Kunitake [23,24]. The effect of solvent polarity on T_g and total melting enthalpy of multi-peaks of PpMS polymers with high molecular weights (M_n = 194,000–258,000 g mol^{-1}) further confirms the crucial factor of tightness in the growing ion pairs in stereospecific cationic polymerization of *p*-methylstyrene.

3.4. Effect of nucleophilicity of amine

The tightness of the growing ion pairs was also increased by introducing triethylamine (TEA) with stronger nucleophilicity or basicity ($pK_{a,TEA}$ = 10.7) than TPA($pK_{a,TPA}$ = −6.4) [36]. Kennedy and Kaszas et al. have proposed the mechanistic role of carbocation stabilization for external strong electron donors or nucleophiles on the living carbocationic polymerization, suggesting that electron donors and/or their complexes with a Lewis acid interact with the growing chain end to reduce its cationicity and thus to convert highly reactive species into less reactive species [1,37]. The electron donor was also proposed to affect the micro-surroundings with more nucleophilicity around the growing species [29]. As expected, PpMS-7 and PpMS-8 obtained in the presence of TEA with stronger basicity had relatively narrow molecular weight distribution (M_w/M_n = 2.5–2.1) in comparison with those in the presence of TPA (M_w/M_n = 2.7–4.1). Strong base TEA might trap H^+ generated by β-H elimination from the growing species during polymerization and then decrease the chain transfer reaction. However, compared to PpMS-3 obtained in the presence of TPA with bulky phenyl groups, PpMS-7 and PpMS-8 had relatively low isotacticity of *P*(mmmm) of 35%, 35% and 33% respectively. Therefore, the crucial factors on the stereochemistry of monomer insertion include both the tightness in the growing ion pairs and the steric hindrance of counteranion in cationic polymerization of *p*-methylstyrene. TEA with stronger basicity mainly contributes to mediate the molecular weight distribution and TPA with larger steric hindrance mainly influences the stereochemistry of monomer insertion. On the other

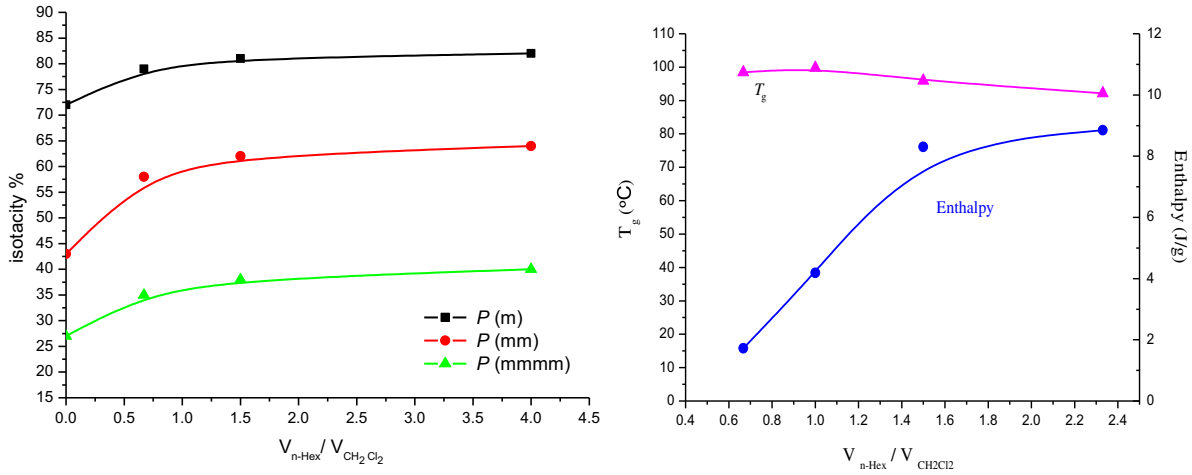

Fig. 7. Effect of solvent polarity on isotacity, T_g and melting enthalpy of poly(*p*-methylstyrene) products. [*p*MS] = 0.5 M, [$AlCl_3$] = 3.8 mM, [TPA] = 1.9 mM, [H_2O] = 0.89 mM, T_p = −80 °C, t_p = 30 min pressure = 10 kg cm^{-1}, T_c = 180 °C.

hand, Storey et al. [38] have theorized that basic additives suppress the concentration of unpaired chain carriers through the in situ production of common ions *via* the scavenging of protic impurities. According to Storey's theory on the mechanistic role of external EDs, the function of the tertiary amine might be also supply common counterions to the system, through water scavenging [38]. This suppresses dissociation of the propagating ion pairs and cause propagation to proceed exclusively through contact ion pairs. The resulting polymers (P*p*MS-7 and P*p*MS-8) also present beautiful crystalline performance in Fig. 8.

3.5. Effect of polymerization temperature

Polymerization temperature is an important factor for the propagation and termination in cationic polymerization. To examine the effect of polymerization temperature, the cationic polymerizations of *p*-methylstyrene with $H_2O/AlCl_3$/TPA initiating system were conducted at various temperatures ranging from −80 to −50 °C. All the experiments got almost complete monomer conversion within 30 min at different polymerization temperatures. The termination and chain transfer reaction will be increased by increasing polymerization temperature, leading to decrease in molecular weight of the resulting polymers, which is a common problem in the conventional cationic polymerization. The inverse effect of polymerization temperature on molecular weights is quantitatively expressed by Arrhenius equation, i.e. $\ln M_n = \ln A - \Delta E/RT$, that is M_n depends on $1/T_p$ [39]. The overall activation energy difference (ΔE or E_{DP}) was calculated to be −14.4 kJ mol^{-1} from the slope of the linear Arrhenius plot of $\ln(M_n)$ vs $1/T_p$ for the temperature interval from −80 to −50 °C, as shown in Fig. 9. On the other hand, the ^{13}C NMR characterization indicates that the two P*p*MS products obtained at −50 °C and −80 °C had almost the same isotacity, i.e. *P*(mmmm), *P*(mm) and *P*(mm) for these two polymers are 38%, 62% and 81% respectively. Therefore, polymerization temperature was not the crucial factor on the stereospecific propagation and stereoregularity of P*p*MS in this polymerization system.

3.6. Mechanism for stereospecific polymerization

Based on the above experimental results and observations, the crystallizable P*p*MS products with more than 75% of m dyad configurations and with very high molecular weights could be prepared *via* the stereospecific cationic polymerization of *p*-methylstyrene initiated by $H_2O/AlCl_3$ in the presence of TPA or TEA. A possible mechanism for stereospecific polymerization of *p*-methylstyrene with $H_2O/AlCl_3$/TPA initiating system was proposed to depict the formation of resulting long polymer chain, as shown in Scheme 1. The propagation proceeded *via* the insertion

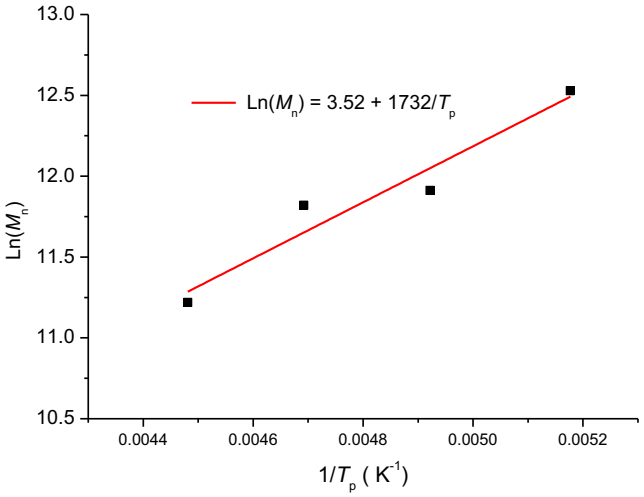

Fig. 9. Arrhenius plot of $\ln(M_n)$ vs $1/T_p$ for cationic polymerization of IB with $H_2O/AlCl_3$/TPA initiating system. [PMS] = 0.5 M; [$AlCl_3$] = 3.8 mM; [TPA] = 1.9 mM; [H_2O] = 0.81 mM; $V_{n-Hex}/V_{CH_2Cl_2}$ = 6/4; t_p = 30 min.

of monomer from the growing ion paired species consisting carbenium ion and counteranion to form high molecular weight polymer chain. The incoming monomer molecules attack the carbonium ion and then polymer chains grow, which depending on both the tightness of the ion paired species and steric hindrance in counteranion. In this polymerization system, counteranion was formed by the combination of Lewis acid ($AlCl_3$) with the anionic part (OH^- or Cl^-) from initiator or the polymer chain terminal and with complex of $AlCl_3$ and nucleophiles (TPA or TEA). The counteranion always associated with the growing carbocation and the tightness of the ion paired species was determined by the distance between carbocation and counteranion, depending on nucleophilicity of amines and solvent polarity. The stereochemical environment of the growing carbocation could be adjusted through designing the tightness of the ion paired species, nucleophilicity and bulkiness of the associating counteranions. The steric course of propagation was mainly determined by the nature of the growing species with appropriate tightness or bulkiness against the monomer insertion and propagation. On the other hand, it has been also pointed out that the conformation of the last two units of the propagating polymer segment and the direction of approach of the incoming monomer would determine the steric course of propagation [25]. The front-side of monomer attack to the carbonium ion gave rise to a syndiotactic placement while the back-side attack of monomer led to isotactic placement [24]. Therefore, the isotactic-

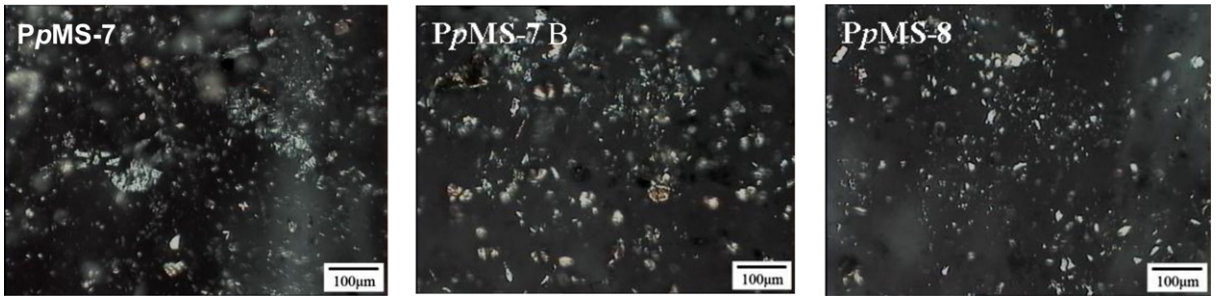

Fig. 8. POM images of P*p*MS-7 and P*p*MS-8 obtained at different concentrations of TEA after flow-induced crystallization under pressure. [PMS] = 0.5 M; [$AlCl_3$] = 3.8 mM, $V_{n-Hex}/V_{CH_2Cl_2}$ = 6/4, T_p = −80 °C, t_p = 30 min. P*p*MS-7: [H_2O] = 1.45 mM, [TEA] = 1.9 mM, Conv% = 20.5%, M_n = 436,000; M_w/M_n = 2.5, *P*(mmmm) = 35%, *P*(mm) = 58%, *P*(*m*) = 79%; P*p*MS-7B: [H_2O] = 0.95 mM, [TEA] = 1.9 mM, Conv% = 63.2%, M_n = 426,000; M_w/M_n = 2.3, *P*(mmmm) = 35%, *P*(mm) = 58%, *P*(*m*) = 79%; P*p*MS-8: [H_2O] = 0.95 mM, [TEA] = 2.3 mM, conversion = 24.6%, M_n = 447,000, MWD = 2.1, *P*(mmmm) = 33%, *P*(mm) = 56%, *P*(m) = 78%. Pressure = 10 kg cm^{-1}, T_c = 180 °C.

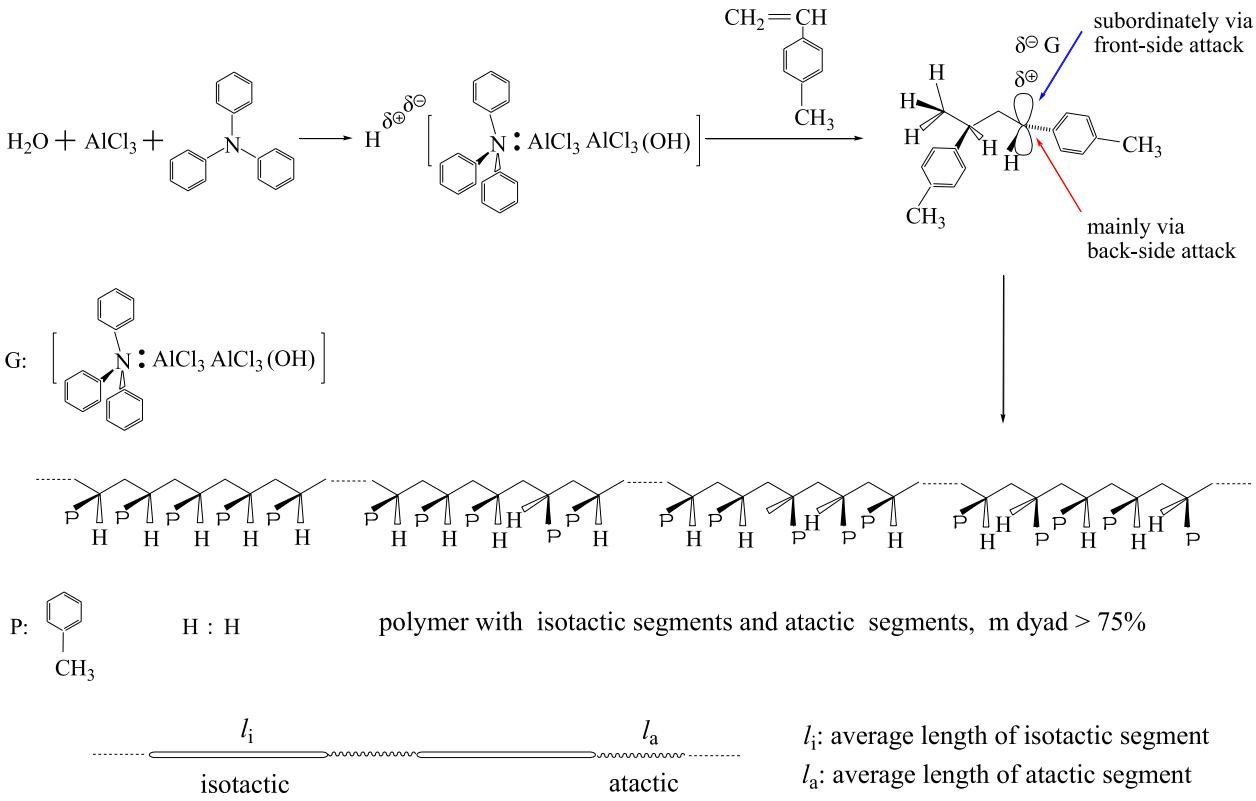

Scheme 1. Possible mechanism for stereospecific cationic polymerization of *p*MS and formation of long polymer chain with isotactic-rich segments.

rich P*p*MS with very high molecular weight could be prepared *via* cationic polymerization by the dominant back-side attack of monomer to the growing ion paired species.

3.7. Model for aligning mechanism

A possible model for the aligning mechanism was sketched to describe the flow-induced crystallization of P*p*MS with several isotactic and atactic segments under pressure at 180 °C, as shown in Fig. 10. After the orientation and arrangement, the polymer chains with isotactic and atactic segments formed crystalline and amorphous regions. The thickness of different lamellaes in crystalline regions was different due to the number and length of isotactic segments, and overlap of some lamellaes.

Moreover, according to the following Gibbs–Thomson equation [40], the melting temperatures of every melting peak in DSC curve for P*p*MS are dependent on the length of isotactic sequences along polymer.

$$\frac{T_{m,i}}{T_{m,o}} = 1 = \frac{2\sigma_e}{l_i \cdot \Delta H_u}$$

where $T_{m,o}$ is the equilibrium melting temperature, $T_{m,i}$ is the melting temperature of each melting peak, σ_e is the basal surface energy of polymer crystals, ΔH_u is the heats of fusion for repeating units, l_i is the length of isotactic sequences for the high molecular weight random copolymer with atactic and isotactic segments.

The crystalline model in Fig. 10 demonstrates the different length, surface and thickness of the crystalline districts, which makes difference in melting temperatures and thus results in multi-melting peaks in DSC curves in Fig. 4.

Furthermore, it can be inferred from the model in Fig. 10 that the free volume of amorphous phases could be enlarged and the entanglement of atactic segments could be decreased due to the

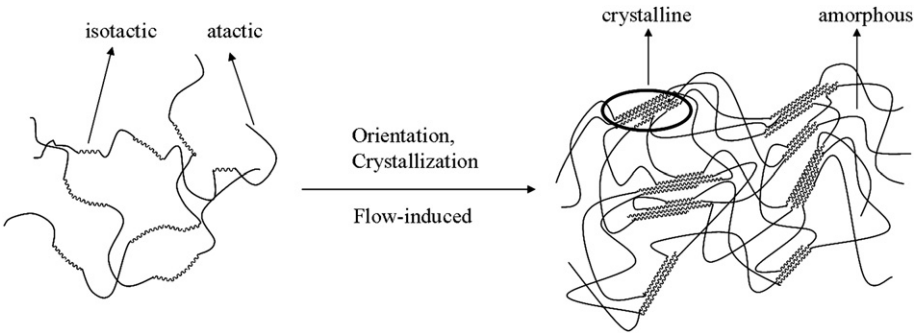

Fig. 10. Possible model for the flow-induced crystallization of isotactic-rich P*p*MS with high molecular weight.

formation of crystalline from the inter- or intra-isotactic P*p*MS segments, leading to facilitate the movement of those atactic P*p*MS segments in amorphous regions and thus lower T_g ($\sim$93 °C) of the above isotactic-rich P*p*MS with high molecular weight than that ($\sim$118 °C) for atactic P*p*MS.

4. Conclusions

The stereospecific cationic polymerizations of *p*-methylstyrene have been achieved with $H_2O/AlCl_3$ initiating system in the presence of triphenylamine or triethylamine. The inverse effect of polymerization temperature on molecular weights was observed and the overall activation energy difference (ΔE or E_{DP}) was calculated to be -14.4 kJ mol^{-1}. The propagation proceeded *via* the dominant back-side attack and insertion of monomer from the growing ion paired species consisting carbenium ion and counteranion to form high molecular weight polymers with isotactic-rich segments along macromolecular chains. The steric course of propagation was mainly determined by the tightness of the growing ion paired species and steric hindrance in counteranions. The bulky triphenylamine with relatively weak nucleophilicity, triethylamine with strong nucleophilicity and solvent polarity did play very important roles in achieving the stereospecific cationic polymerization of *p*-methylstyrene for their contributions to the ion paired species. Polymerization temperature was not the crucial factor on the stereospecific propagation and stereoregularity of P*p*MS. The resulting isotactic-rich poly(*p*-methylstyrene) with high molecular weight, having high meso dyad (m) content of more than 75% could form crystal morphology with 10–30 μm in size by flow-induced crystallization under pressure at 180 °C. A possible model for the aligning mechanism was sketched to describe the flow-induced crystallization of P*p*MS with several isotactic and atactic segments and to explain the multi-melting peaks and lower glass transition temperatures. Further investigations will be done along this line in our laboratory.

Acknowledgments

The financial supports from National Natural Science Foundation of China (Grant 20934001) and National Basic Research Program of China (973 Program, 2011CB606002) are greatly appreciated.

References

[1] Kennedy JP, Ivan B. Designed polymers by carbocationic macromolecular engineering. New York: Hanser Publishers; 1992.
[2] (a) Faust R, Kennedy JP. Polym Bull 1988;19:21–8;
(b) Faust R, Kenndy JP. Polym Bull 1988;19:29–34;
(c) Fodor Z, Gyor M, Wang HC, Faust RJ. Macromol Sci Pure Appl Chem 1993; A30:349–63.
[3] (a) Kaszas G, Puskas JE, Kennedy JP, Hager WG. J Polym Sci Part A Polym Chem 1991;29:421–6;
(b) Puskas JE, Chan SWP, McAuley KB, Kaszas G, Shaikh S. J Polym Sci Part A Polym Chem 2007;45:1778–87.
[4] Smith QA, Storey RF. Macromolecules 2005;38:4983–8.
[5] (a) Kojima K, Sawamoto M, Higashimura T. J Polym Sci Part A Polym Chem 1990;28:3007–17;
(b) Ishihama Y, Sawamoto M, Higashimura T. Polym Bull 1990;24:201–6;
(c) Higashimura T, Ishihama Y, Sawamoto M. Macromolecules 1993;26: 744–51;
(d) Hasebe T, Kamigaito M, Sawamoto M. Macromolecules 1996;29:6100–3.
[6] Yang ML, Li K, Stover HDH. Macromol Rapid Commun 1994;15(5):425–32.
[7] Nagy A, Majoros I, Kennedy JP. J Polym Sci Part A Polym Chem 1997;35(16): 3341–7.
[8] (a) Kostjuk SV, Kapytsky FN, Mardykin VP, Gaponik LV, Antipin LM. Polym Bull 2002;49:251–6;
(b) Kostjuk SV. Polym Bull 2004;51:277–83;
(c) Kostjuk SV, Ganachaud F. Macromolecules 2006;39:3110–3;
(d) Kostjuk SV, Dubovik AYu, Vasilenko IV, Frolov AN, Kaputsky FN. Eur Polym J 2007;43:968–79;
(e) Frolov AN, Kostjuk SV, Vasilenko IV, Kaputsky FN. J Polym Sci Part A Polym Chem 2010;48:3736–43.
[9] Banerjee S, Paira TK, Kotal A, Mandal TK. Polymer 2010;51:1258–69.
[10] Lin CH, Xiang JS, Matyjaszewski K. Macromolecules 1993;26:2785–90.
[11] Kwon OS, Kim YB, Kwon SK, Choi BS, Choi SK. Makromol Chem 1993;194: 251–75.
[12] Aoshima S, Segawa Y, Okada Y. J Polym Sci Part A Polym Chem 2001;39: 751–5.
[13] Kennedy JP, Thomas RM. Makromol Chem 1962;53:28–32.
[14] Kennedy JP. J Polym Sci Part A Polym Chem 1999;37:2285–93.
[15] Okamura S, Higashimura T, Watanabe T. Makromol Chem 1961;50:137–46.
[16] Yuki H, Hatada K, Ota K, Kinoshita I, Murahashi S, Ono K, et al. J Polym Sci Part A Polym Chem 1969;7:1517–36.
[17] Sikkema DJ, Angad-Gaur H. Makromol Chem 1980;181:2259–66.
[18] Angad-Gaur H, Sikkema DJ. Makromol Chem 1980;181:2385–93.
[19] Ohgi H, Sato T. Macromolecules 1993;26:559–60.
[20] Ouchi M, Kamigaito M, Sawamoto M. Macromolecules 1999;32(20):6407–11.
[21] Ouchi M, Kamigaito M, Sawamoto M. J Polym Sci Part A Polym Chem 2001; 39(7):1060–6.
[22] Kanazawa A, Kanaoka S, Aoshima S. J Polym Sci Part A Polym Chem 2010;48: 3702–8.
[23] Higashimura T, Yonezawa T, Okamura S, Fukui K. J Polym Sci 1959;39:487–92.
[24] Kunitake T, Aso C. J Polym Sci Part A 1 Polym Chem 1970;8:665–78.
[25] Kunitake T, Takarabe K. Makromol Chem 1981;182:817–24.
[26] Stenzel O, Brüll R, Wahner UM, Sanderson RD, Raubenheimer HG. J Mol Catal A Chem 2003;192:217–22.
[27] Vijayaraghavan R, MacFarlane DR. Macromolecules 2007;40:6515–20.
[28] Bueno C, Cabral VF, Cardozo-Filho L, Dias ML, Antunes OAC. J Supercritical Fluids 2009;48:183–7.
[29] (a) Wu YX, Tan YX, Wu GY. Macromolecules 2002;35:3801–5;
(b) Li Y, Wu YX, Xu X, Liang LH, Wu GY. J Polym Sci Part A Polym Chem 2007; 45:3053–61.
[30] Frisch HL, Mallows CL, Bovey FA. J Chem Phys 1966;45:1565–77.
[31] Lu XY, Jiang BZ. Acta Polym Sin 1990;5:532–7.
[32] Teng HX, Shi Y, Jin XG. J Polym Sci Part A Polym Chem 2002;40:2107–18.
[33] Elmoumni A, Winter HH, Waddon AJ. Macromolecules 2003;36:6453–61.
[34] Kawamura T, Uryu T, Matsuzaki K. Makromol Chem 1982;183:125–41.
[35] Zhang X, Yan W, Li H, Shen X. Polymer 2005;46:11958–61.
[36] (a) Kaljurand I, Kutt A, Soovali L, Rodima T, Maemets V, Leito I, et al. J Org Chem 2005;70:1019–28;
(b) Oss M, Kruve A, Herodes K, Leito I. Anal Chem 2010;82:2865–72.
[37] (a) Kaszas G, Puskas JE, Kennedy JP. J Macromol Sci Chem 1989;26:1099–114;
(b) Kaszas G, Puskas JE, Chen CC, Kennedy JP. Macromolecules 1990;23: 3909–15;
(c) Kennedy JP, Majoros I, Nagy A. Adv Polym Sci 1994;112:1–114.
[38] Storey RF, Curry CL, Hendry LK. Macromolecules 2001;34:5416.
[39] (a) Kennedy JP. Cationic polymerization of olefins: a critical inventory. New York: Wiley Interscience; 1975. p. 113;
(b) Thomas RM, Sparks WJ, Frolich PK, Otto M, Muller-Cunradi M. J Am Chem Soc 1940;62:276–80;
(c) Flory PJ. In: Principles of polymer chemistry. Ithaca, New York: Cornell University Press; 1953. p. 218;
(d) Kennedy JP, Marechal E. Carbocationic polymerization. New York: Wiley; 1982. pp. 197–225.
[40] Wunderlich B. Macromol Phys 1980;3. Academic: New York.